Cluster-cluster aggregation in two-monomer systems

1986 J. Phys. A: Math. Gen. 19 2137

(http://iopscience.iop.org/0305-4470/19/11/023)

J. Phys. A: Math. Gen. 19 (1986) 2137-2153. Printed in Great Britain

Cluster–cluster aggregation in two-monomer systems

Paul Meakin† and Zoran B Djordjević‡

† Central Research and Development Department, EI du Pont de Nemours and Company, Inc, Experimental Station, Wilmington, Delaware 19898, USA

‡ 'Boris Kidrič' Institute of Nuclear Science, Laboratory for Solid State Physics and Radiation Chemistry, PO Box 522, 11001 Belgrade, Yugoslavia

Received 6 June 1985, in final form 10 October 1985

Abstract. We have investigated the structure and growth kinetics of clusters formed in dilute solutions from two kinds of polyfunctional monomers. This was done by computer simulations within the framework of the cluster-cluster aggregation model with mass-independent cluster diffusion constants. The systems considered were of the type A_2+B_f and A_f+B_f, where A_2, A_f and B_f are different monomers. The monomer functionality f is equal to the coordination number of the lattice used in the simulations. The results of simulations obtained at different relative monomer concentrations are described and several novel effects are reported. Large clusters always have a fractal-like geometry but their effective fractal dimensionality, D, appears to depend on the composition of the mixture. Only in a restricted composition range does the aggregation process lead to a single large cluster. There, the cluster size distribution function $N_s(t)$ can be described by the scaling form $s^{-2}f(s/t^z)$. Outside this range, aggregation results in small clusters (oligomers) whose structure is governed by 'geometric selection rules'. Only certain non-consecutive oligomer weights are observed. The two boundary points of the interval in which kinetic scaling holds are shown to possess the properties of tricritical points.

1. Introduction

Considerable interest has recently been generated in non-equilibrium growth and aggregation models which simulate phenomena such as polymerisation and gelation, colloidal aggregation, dendrite formation and a variety of biological processes. Much of this interest was stimulated by the discovery of Witten and Sander (1981) that a simple diffusion-limited aggregation model in which particles are added one at a time via random walk trajectories to a growing cluster or aggregate of particles generates structures with a well defined fractal dimensionality (D) (Mandelbrot 1982), distinctly smaller than the Euclidean dimensionality (d) of the space or lattice used in the simulation. The work of Witten and Sander demonstrated that it may be possible to understand the tenuous fractal-like structures of many natural objects by analysing *simple* aggregation models. However, the Witten-Sander model is not a realistic representation of colloidal aggregation. A more realistic model incorporating both particle-particle and cluster-cluster addition processes as well as particle-cluster aggregation was recently introduced by Meakin (1983) and Kolb *et al* (1983). This model leads to structures which have a considerably smaller fractal dimensionality than those generated by the Witten-Sander model. The cluster-cluster aggregation model combines some of the features of both the Witten-Sander model and the earlier Sutherland and Goodarz-Nia (1971) model in which clusters are brought together via

0305-4470/86/112137+17$02.50

linear rather than random walk trajectories. The cluster-cluster aggregation model leads to structures which closely resemble those observed in certain metal particle aggregates (Forrest and Witten 1979, Weitz and Oliveria 1984). In other cases, naturally occurring aggregation processes lead to structures with a somewhat higher fractal dimensionality than that found in computer simulations based on the cluster-cluster aggregation model. This may be the result of small sticking probabilities (Kolb and Jullien 1984) or other effects such as the reorganisation after the initial aggregation process which are now being investigated by computer simulation (Meakin and Jullien 1986).

Initially, the interest in these aggregation models focused on the fractal geometry of the generated structures. More recently, attention has been directed towards the growth process itself (Racz and Plishke 1984, Meakin and Witten 1983) and, in particular, the kinetics of the growth process (Meakin *et al* 1985b). Friedlander (1960, 1977) and other workers in aerosol science (Lushikov 1973) and astronomy (Silk and White 1978) have pointed out that kinetic aggregating systems possess a scaling symmetry which involves the aggregation time and manifests itself by the existence of a characteristic cluster size growing as a power law in time. In these systems $N_s(t)$, the number of clusters of size s, at time t, can be expressed as

$$N_s(t) \sim s^{-2} f(s/t^z) \tag{1}$$

where $f(x)$ is a scaling function and z is a scaling exponent. As a result, the concept of 'self-preserving cluster size distributions' has become a part of colloid science. For the case of cluster-cluster aggregation, scaling form (1) has been obtained by Botet and Jullien (1984) using Smoluchowski equations and by Vicsek and Family (1984) and Kolb (1984) who have shown that it describes the results of Monte Carlo simulations. The same scaling form has been found in other kinetic models (Kang and Redner 1984).

Work carried out during recent months (Deutsch and Meakin 1983, Botet and Jullien 1984) has shown how the scaling exponent z and scaling function $f(x)$ are related to the fractal dimensionality D and the exponent γ, the latter describing the dependence of the cluster diffusion coefficient $D(s)$ on the cluster size ($D(s) \sim s^{\gamma}$). In the cluster-cluster aggregation model γ is treated as an independent parameter, though in real systems it must be related to the fractal dimension D (Meakin *et al* 1985a).

The kinetics of polymerisation reactions is a well established field (Flory 1953). However, it is only with the realisation that polymers are fractals that the effects of geometry on the kinetics of dilute polymerising systems has come to be fully appreciated. In the classical kinetic theory of polymerisation, the temporal evolution of the total number of reactive groups is calculated assuming that any reactive group is capable of reacting with any other appropriate reactive group anywhere in the solution. The location of a reactive group on the 'surface' or 'interior' of the growing molecule or cluster is believed to be irrelevant. This assumption of 'equal reactivity' of chemical groups is partially justified in dense solutions and melts but is an obvious over-simplification for the processes in dilute solutions where the average distance between clusters is comparable to or larger than the average radius of the clusters. For the case of two rigid fractal structures with the same fractal dimensionality, the equal reactivity assumption will be correct only if the two fractals are mutually transparent. The condition for mutual transparency (Ball and Witten 1983) is

$$2D + D_w < d \tag{2}$$

where D_w is the fractal dimensionality of the trajectory or walk describing the relative motion of the two clusters. D_w has a value of 2 for diffusion (Brownian trajectory) and 1 for a linear trajectory and an *effective* value of 0 for a Brownian trajectory in the limit of low chemical reactivity or sticking probability. However, the inequality given in (2) is not satisfied by real two- or three-dimensional systems. For example, in three-dimensional cluster–cluster aggregation $2D = 3.5$ and clusters are not transparent. This absence of transparency means that clusters collide through contact of their surfaces and their interiors are effectively screened. Consequently, we expect to find a very broad distribution of reactivities, varying from zero, for completely inaccessible interior groups, to very large values, for groups at very exposed locations. This broad distribution of reactivities is, in fact, essential for the formation of fractal structures in the first place. If all groups were equally reactive, the interior of the cluster would also grow and we would have a much denser structure. In principle, the equal reactivity assumption is inadequate whenever geometric (spatial) effects are important. Still, it is extensively used to predict the time dependence of observable quantities such as the number of clusters, their average mass and the number of 'bonds' formed in polymerisation processes. In general, this assumption leads to results quite different from those obtained from scaling theories which include the effects of geometry on the availability of reactive groups (Ziff *et al* 1982). The latter theories predict power law behaviour for the above mentioned observables as functions of the reaction time, in sharp contrast to linear or exponential functions typically predicted by the equal reactivity models. Most real systems lie somewhere between the extremes represented by the equal reactivity models and the cluster–cluster aggregation model.

In this paper, we present results of the lattice cluster–cluster aggregation model with two types of monomers which automatically includes the effects of geometry on the availability of reactive sites. We will also show that, under certain conditions, the time-dependent cluster size distributions in this two-monomer model satisfy equation (1).

Most of the results presented below are verified by all four types of system considered. In order to avoid being repetitious, each general statement is illustrated by one example on a specific system.

2. Aggregation in two-monomer systems

Almost all simulations of non-equilibrium growth and aggregations have been carried out under the assumption that all of the monomers are identical and, in the case of lattice model simulations, have a functionality equal to the coordination number of the lattice. In the off-lattice simulations of colloidal processes, it is usually assumed that the particles are hyperspherical and may stick at any contact point. Polymerisation reactions, however, frequently involve two monomeric species of the type A_g and B_f where g and f are the monomer functionalities. In contrast to single-monomer aggregation, bonds in $A_g + B_f$ systems are formed between the unlike chemical groups only.

Practically all gel-forming polycondensation processes (Flory 1953) are of this latter kind, where one of the monomers is usually two-functional. Aggregation of antigen coated latex spheres and two-functional antibody molecules (von Schulthess *et al* 1980) is an example of the $A_2 + B_f$ system with a very large value of f. Some biological processes such as the self-aggregation of proteins (Feder *et al* 1984), which are often presented as single-monomer aggregations, may also be regarded as examples of the

two-monomer systems, since the hydrogen ions which are invariably the mediators of the hydrogen bonds can be envisaged as A_2 reagents. The aggregation in two and multicomponent mixtures is obviously of sufficient practical importance to warrant a detailed study.

In a single-monomer B_f system, the concentration of B_f molecules is the only non-thermal parameter that controls the reaction rate. The presence of two independent concentrations in an $A_g + B_f$ system suggests that both the overall concentrations of two monomers and their relative concentration are important variables. This can be easily seen in the extreme case of polymerisation with the overabundance of one component. The reaction will rapidly produce clusters, the surface elements of which are predominantly of one type. Further collisions of these clusters will bring into contact only chemical groups of that one type and the reaction will terminate, irrespective of the overall concentration of the two components. The marked imbalance of the chemical species therefore prevents the reaction from forming large molecules and that is why most polymerisations are performed at equal concentrations of reactive groups. This practice unfortunately leads to the belief that kinetic theories with a single reaction coordinate (Flory 1953) are sufficient to describe two-component systems. Of course it is easier to construct the former theories and it is important to understand whether and under what conditions the two-component and the single-component systems exhibit the same physical behaviour. Also, the aggregation in the $A_2 + B_f$ systems resembles the site-bond percolation problem (Nakanishi and Reynolds 1978, Kinzel and Yeomans 1981) where the A_2 molecules serve as bonds between the B_f branching sites. This correspondence needs to be examined and it should be seen whether the numerous results of percolation theory can be adapted to this particular class of aggregation processes.

Another important aspect of these models is the possibility that the effective fractal dimensionality may depend on the relative concentration of the two components. If this is the case, the effective kinetic exponent, z, may also depend on the concentration ratio.

In this paper we describe some of the results obtained from computer simulations. A companion paper (Djordjević and Meakin 1986) examines the same two-monomer models using the classical Flory-Stockmeyer approach.

3. Computer model

We performed simulations on a two-dimensional square lattice and a three-dimensional cubic lattice with periodic boundary conditions. In both dimensions, we considered two classes of monomer pairs: $A_f + B_f$ and $A_2 + B_f$. Most real polymerisation processes leading to branched polymers and gels utilise A_2 and B_3, B_4 or B_∞ monomers. We believe that qualitative pictures will not change appreciably for different functionalities, f, and present the most convenient models with f equal to the coordination number of the lattice, in $d = 2$, $f = 4$ and in $d = 3$, $f = 6$. In all cases, the diffusivity of the clusters and monomers is taken to be mass independent. A more realistic model with a mass-dependent diffusion coefficient will be considered in future work. Also, we considered different initial concentration ratios. Most frequently, we refer to the relative proportion of the two species either by the number fraction of the A_g component or by the ratio r of the number of chemical groups

$$r = gA_g/fB_f. \tag{3}$$

Since we believed that the scaling form (1) of the cluster size distribution function applies to dilute aggregation systems, we worked with monomer concentrations in the range 0.2–1.5%. Further decrease in the concentration would cause serious degradation in the statistical quality of the data or increase the computer time unreasonably.

At the beginning of a simulation, a certain number of A_g monomers is distributed randomly on the lattice and if they are of the A_2 type, they are randomly oriented. Subsequently, a number of B_f monomers corresponding to the desired ratio r are randomly placed among the vacant sites. At each step in the simulation a molecule is picked at random and moved by one lattice unit in a randomly chosen direction. Every movement of a molecule increments the reaction time by $1/N(t)$, where $N(t)$ is the number of molecules (monomers and polymers) on the lattice. Translational motion of an A_2 molecule is accompanied by a random rotation. Translation is the only allowed motion for clusters of two or more monomers. If two clusters make contact and a properly oriented A group on one cluster finds itself adjacent to a B group on the other, the two clusters permanently join. If two clusters make contact via an AB pair in which the A group is not correctly oriented for reaction, they are allowed to remain in contact but are not joined. If an attempted translation of a cluster would cause it to overlap one or more adjoining clusters, the attempted move is not permitted but the time is incremented by $1/N(t)$, i.e. time is defined in units of *attempted* moves per cluster. Occasionally, more than one cluster will simultaneously come in contact. In this event all new contacts are examined for the monomer type and orientation, and 'bonds' are formed between all properly oriented contacting A and B groups. As the simulation proceeds, collisions between clusters result in the formation of larger clusters. The total number of clusters, N_0, is continuously monitored. The weight average molecular weight $S(t)$ given by $S(t) = N_0^{-1}\Sigma_s s^2 N_s(t)$, where N_0 is the total number of monomers in the system, is also monitored. The cluster size distribution is established and stored for further analysis 100 times during the simulation. For convenience, both types of monomers are assumed to have equal mass. Clusters are characterised only by their total mass and not by the separate numbers of A_g and B_f monomers they contain. In order to obtain reasonably good statistics for the time-dependent cluster size distribution, it is necessary to average the results from a number of simulations (typically 5–50).

4. Reaction rate as a function of composition field

To illustrate the structure of the clusters obtained in two-monomer systems, the result of a small scale simulation on a 64×64 periodic lattice involving 500 particles with an equal proportion of A_4 and B_4 monomers is shown in figure 1. The clusters appear very ramified and resemble those obtained on the basis of simple cluster-cluster aggregation models. The A_4 and B_4 monomers are represented as black and white squares, respectively. Every edge of a square represents a functional group of the corresponding type. Note the checkerboard arrangement in which every square only has opposite nearest neighbours.

In order to obtain an improved picture of the fractal character of the aggregates, several large scale simulations on a 512×512 lattice with 8000 particles were performed. In figure 2(a) we present the symmetric 50/50 case. Note the highly ramified structure. The two types of monomers cannot be distinguished on this scale. The result of another simulation with approximately twice as many B_4 as A_4 monomers is presented in figure

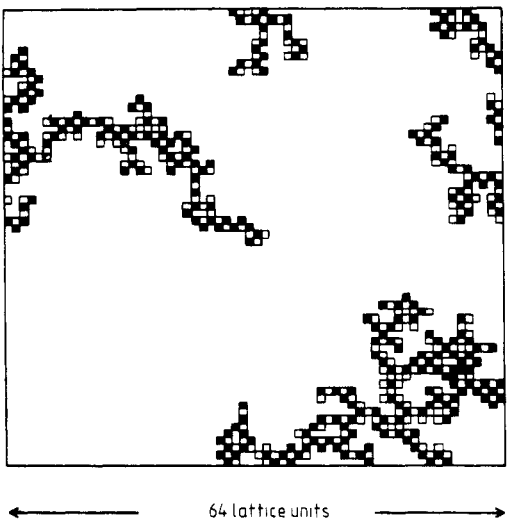

Figure 1. Small scale simulation of A_4+B_4 aggregation on a 64×64 square lattice with 500 particles. The cluster is a fully grown 'micro-gel'. The initial monomer ratio is 50/50.

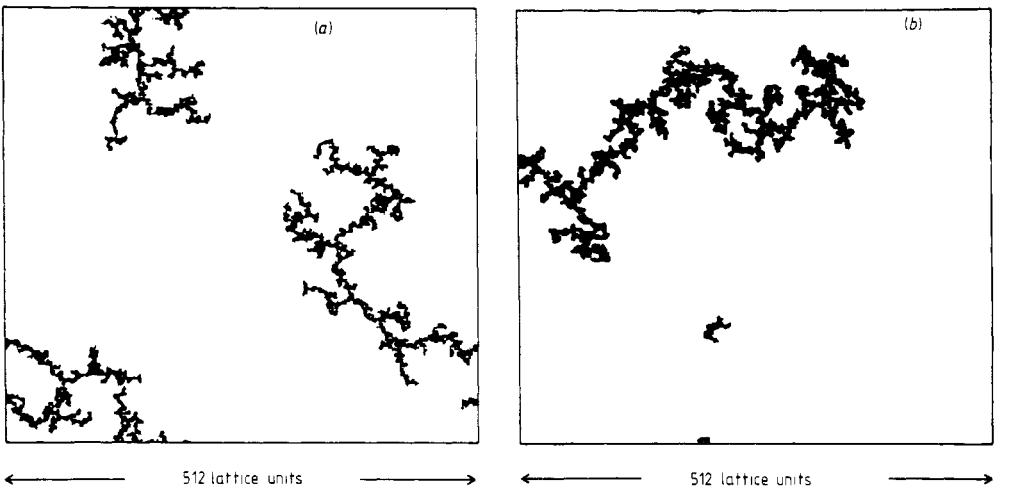

Figure 2. (*a*) Final cluster in a large scale A_4+B_4 simulation on a 512×512 square lattice with periodic boundary conditions and 8000 particles. The initial monomer ratio is 50/50. (*b*) Result of the aggregation in an A_4+B_4 system on a square 512×512 periodic lattice with 8000 particles and an initial concentration ratio: 32.5/67.5.

2(*b*). The aggregation process, up to the point presented in this picture, proceeded for 8 h CPU time on an IBM 3081 computer. This is approximately 10 times longer than for the process in figure 2(*a*). However, the system is not fully aggregated and beside the one large cluster, three small clusters are visible. The test of whether this particular configuration would ever completely aggregate would require considerable computer time and was not attempted. A comparison of two large clusters of figures 2(*a*) and 2(*b*) shows the 'considerably' higher compactness of the latter.

The chemical composition of the mixture clearly influences the reaction rate and, at least in the case of A_4+B_4 systems, asymmetry in the composition slows the reaction

down. To investigate this observation in a more quantitative manner, simulations have been carried out at different relative monomer concentrations using all four models. If a particular mixture fully aggregates into a single large cluster we call it a 'gelling mixture'. A composition which does not result in a single cluster after a 'long' aggregation time is classified as 'non-gelling'. We have chosen an arbitrary value, $S = 100$ monomer masses, and recorded the reaction time at which the weight average molecular weight reaches that value. Plots of the reaction time against composition for all four models are given in figure 3. These curves are similar to the gelation curves of our companion paper (Djordjević and Meakin 1986) where we calculated gelation time as a function of the ratio r. The physical implications of the gelation diagrams and figure 3 of this paper are practically the same.

Figure 3 shows that optimal compositions exist at which the reactions proceed most rapidly. In the case of $A_f + B_f$ systems these compositions are naturally placed at $X = 50\%$. What is particularly interesting is that the optimal compositions in the $A_2 + B_f$ mixtures do not coincide with the equivalent compositions ($r = 1$) which have the same number of A and B chemical groups. The equivalent compositions in the case of $A_2 + B_4$ and $A_2 + B_6$ systems contain 66% and 75% of A_2 monomers respectively. However, the optima in our simulations are considerably below these values. Apparently, the intuitive assumption that the $A_g + B_f$ system polymerisation ($g \neq f$) is

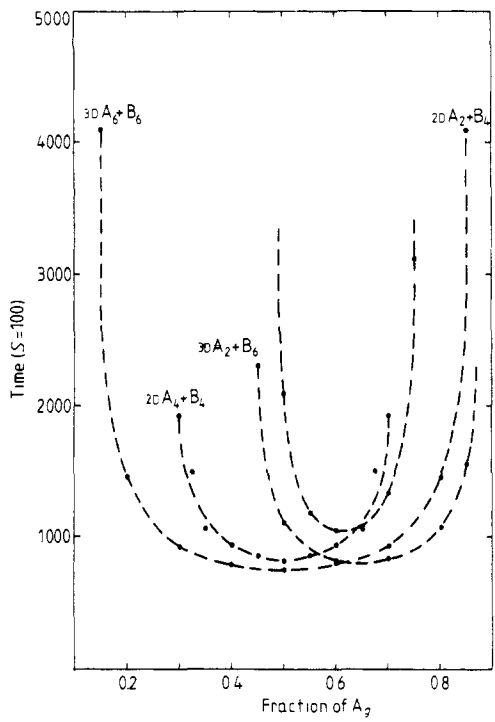

Figure 3. Reaction time necessary for systems of 10 000 A_g and B_f monomers on an appropriate two- or three-dimensional lattice to reach a mean cluster size $S = 100$ as a function of the fraction of A_g monomers. S is the weight average molecular weight in units of monomer mass. The results were obtained by averaging over a number of simulations. The reader should note that the data for $A_f + B_f$ systems will not appear symmetric around the $X = 0.5$ axis, if presented as functions of ratio r.

optimised if the two chemical groups are equally numerous is not supported by our simulations. The same conclusion may be drawn from our classical theory of these phenomena (Djordjević and Meakin 1986).

Results of our simulations indicate not only that the reaction time increases as we change the composition away from the optimal but also that it diverges at two finite values: $X_{\min}(r_{\min})$ and $X_{\max}(r_{\max})$. This is in full agreement with the previous theoretical results (Djordjević 1984). Here we performed only a partial analysis of these divergencies, deeming it more important to present the complete phenomenology of the processes first.

5. Existence of kinetic scaling in two-monomer systems

The existence of scaling in kinetic aggregation processes has attracted considerable interest (Vicsek and Family 1984, Botet and Jullien 1984) recently and it is natural to examine the effects of the presence of two monomers on this scaling. We are aware that scaling behaviour can be influenced by the value of the diffusion constant exponent γ but in this paper we did not attempt simulations with values of γ other than zero. Also, as we are not simulating any particular chemical reaction, we have assigned the same mass to both monomers. The molecular weight of a particular polymeric molecule is then equal to the number of monomers of either type.

The cluster size distribution function $N_s(t)$ for a two-dimensional A_4+B_4 system with a 50/50 monomer ratio is presented as a $\ln(N_s(t))$ against $\ln(t)$ plot of figure 4. Examining it from top to bottom, we see the time evolution of the number of monomers, dimers, trimers, etc. If the function $N_s(t)$ assumes the scaling form $s^{-2}f(s/t^z)$ then quantity $s^2N_s(t)$, when plotted against $x=s/t^z$, should (for different times t) follow the universal curve, $f(x)$. A result of this reduction of data is presented in figure 5 for six consecutive times t. The data are collapsed by adjusting the scaling exponent z to the value $z=1.3$. The slight dispersion of the curves apparent in figure 5 is a natural consequence of the limitations inherent in the simulation methods and does not necessarily indicate inadequacy of the scaling form. It is interesting to note that the same value of exponent z is obtained in the cluster-cluster aggregation model with one monomer and diffusivity exponent $\gamma=0$ (Meakin *et al* 1985b). Another confirmation of the applicability of the above scaling form is given in figure 6, where we present

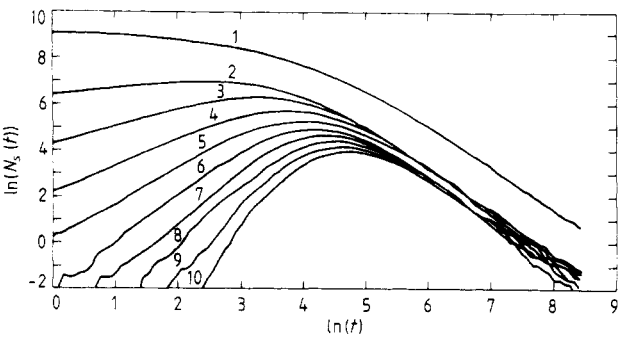

Figure 4. Time evolution of the number of small clusters of sizes 1-10, during simulations carried out on a 512×512 lattice with 10 000 particles in a 2D 50% $A_4+50\%$ B_4 system with symmetric monomer composition. $D(s)\sim s^0$.

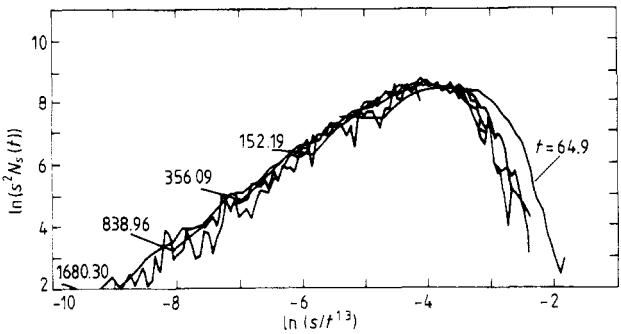

Figure 5. Reduction of the cluster size distribution function $N_s(t)$ to the universal scaling function $f(s/t^z)$ for a symmetric 2D (50% A_4+50% B_4) system. Each curve corresponds to a particular time t. Collapse of data is better for higher reaction times. The curve with the lowest time presented, $t=64.9$, deviates from the rest of the data.

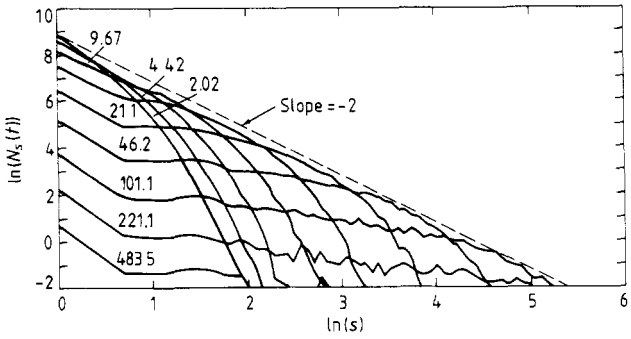

Figure 6. Cluster size distribution function $N_s(t)$ as a function of s at different reaction times t for 2D 50% A_4+50% B_4. Note the slope of the envelope of these curves which is equal to -2. This is a confirmation that $N_s(t)$ possesses a scaling form: $N_s(t) \sim s^{-2}f(s/t^z)$.

$\ln(N_s(t))$ as a function of $\ln(s)$ for several values of t. The envelope of this set of curves follows a straight line with a slope of -2. For every t, labelling one of these curves, we may choose a point on the curve with a value of s such that s/t^z is equal to a prescribed constant y. A value of $N_s(t)$ equal to $s^{-2}f(y)$ corresponds to every such point. Since $f(y)$ is a constant, all these points, in a double logarithmic diagram in figure 6, must lie on a straight line with a slope of -2. The envelope of the curves in figure 6 is just one such set of points.

The scaling for $N_s(t)$ implies that colligative properties such as the mean number of clusters or mean molecular weight of clusters grow as powers of time t. In figure 7 we present a double logarithmic plot of the mean number of clusters N as a function of time t obtained from a three-dimensional system with 80% A_2 and 20% B_6 molecules. After an initial 'crossover' period, the curve approaches a straight line, i.e. the mean number of clusters N falls as a power of the reaction time. Similar behaviour is observed in figure 8 where we present the second moment of the cluster size distribution $S(t)$, which is proportional to the weight average molecular mass of the clusters. Again, the function approaches a straight line, the slope of which in the ln-ln plot equals the scaling exponent $z=2.5$. Due to finite-size effects, both of the last two curves will flatten into horizontal lines with values $N=1$ and $S=N_0$ respectively, where N_0 is the number of particles in the system. This happens immediately after the region

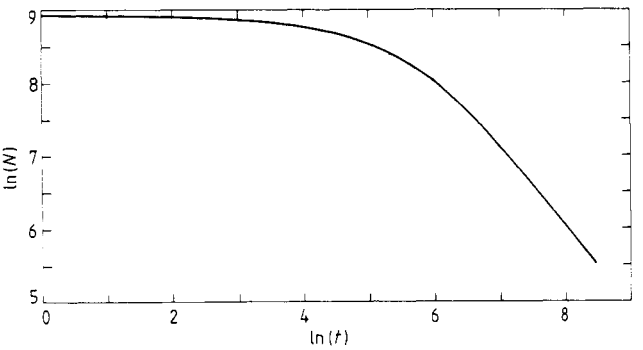

Figure 7. Mean number of clusters as a function of reaction time in a 3D 80% $A_2+20\%$ B_6 system. At large times function $N(t)$ becomes a straight line on this ln-ln plot, indicating a power law behaviour. These and other three-dimensional simulations are carried out using a total of 10 000 monomers on a 128^3 lattice.

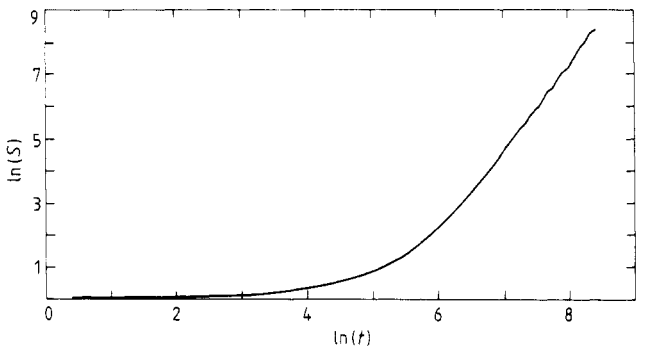

Figure 8. Weight average molecular weight $S(t)=\Sigma_s s^2 N_s(t)/\Sigma_s s N_s(t)$ obtained for a three-dimensional 3D 80% $A_2+20\%$ B_6 system. After an initial non-scaling region, $S(t)$ grows as a power of t.

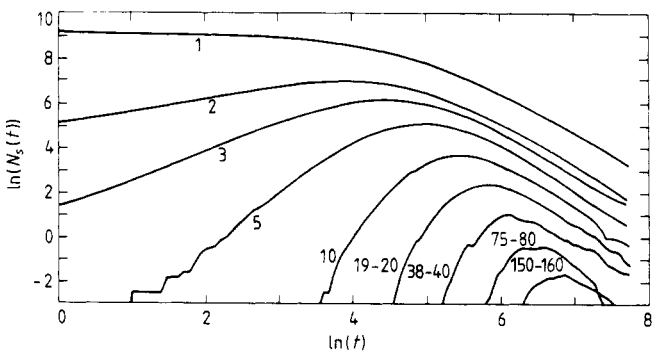

Figure 9. Time evolution of the number of clusters in a 3D 50% $A_6+50\%$ B_6 system of symmetric composition.

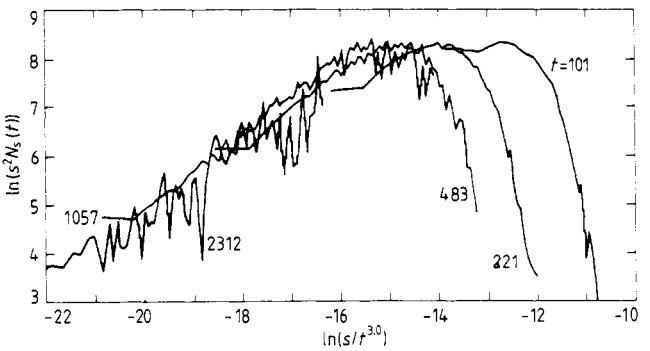

Figure 10. The results of an attempt to scale the cluster size distribution functions obtained at various times in simulations of a three-dimensional 50% A_6 + 50% B_6 system. The best collapse of the data into a single curve is obtained with an exponent z of close to 3.0.

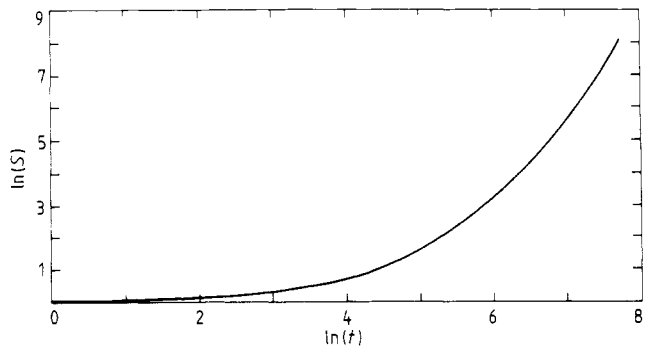

Figure 11. Time dependence of the weight average molecular weight obtained from the three-dimensional simulations of a 3D 50% A_6 + 50% B_6 system at equal concentrations of the two monomers. The results are deduced from the data presented in figure 10.

presented in these graphs. Other graphs in which this finite-size effect is clearly visible are presented in figure 13 below.

In figure 9, we present the time evolution of several cluster sizes in a three-dimensional $A_6 + B_6$ system with equal amounts of two monomers. The result of the collapse of data as presented in figure 10 is unfortunately not very convincing. The closest we can come to a full collapse is achieved with the value of $z = 3.0$. A partial explanation of the difficulties can be inferred from the plot of the second moment of the cluster size distribution given in figure 11. The curvature of this graph is very pronounced and it is impossible to determine the scaling region. From our experience with single-component systems (Meakin *et al* 1985b), we know that this is a consequence of finite concentration effects which are very pronounced in systems with diffusivity exponent $\gamma > 0$. We expect that the scaling form for $N_s(t)$ will be applicable with much greater accuracy in systems with $\gamma < 0$.

6. Tricriticality and the role of the composition field

We have already shown that changes in the composition of the initial monomer mixture influence the kinetics of polymerisation. Going back to figure 2, we see that, besides

strongly affecting the reaction rate, the composition affects the structure of the clusters as well. In this particular example, clusters formed in the asymmetric mixture (figure 2(*b*)) appear more compact than the cluster formed in the symmetric mixture (figure 2(*a*)). To quantify these observations we have analysed the fractal structure of aggregates obtained at two different compositions: 50/50 and 35/65 of an A_4+B_4 system. The effective fractal dimension D is determined by two independent methods. These effective dimensionalities are obtained from the geometric scaling relationships

$$R_g(s) \sim s\beta \qquad \beta = 1/D_\beta \tag{4}$$

and

$$C(R) \sim R^{-\alpha} \qquad \alpha = d - D_\alpha. \tag{5}$$

In equation (4), $R_g(s)$ is the radius of gyration of polymers of mass s. In equation (5), $C(R)$ is the two-point density-density correlation function, R is the distance and d is the ordinary, Euclidean, dimensionality of the lattice in which the system is embedded.

In both cases, five simulations were carried out using 8000 particles on 512×512 lattices. The results are presented in figure 12 and table 1, respectively. Both methods of measurement of the fractal dimension give results which agree within the given error limits. Here and throughout this paper the error limits are the 95% confidence range and only include the contribution of statistical uncertainties. Systematic errors may be larger. The asymmetric aggregates have a fractal dimension $D = 1.53 \pm 0.05$ which is higher than the fractal dimension $D = 1.46 \pm 0.02$ of the symmetric aggregates. This implies that the effective fractal dimension of clusters depends on the composition of the monomer mixture. To examine the dependence of the kinetic exponent z on the initial monomer composition we recorded the time evolution of the second moment, $S(t)$, for five different compositions of an A_4+B_4 system. The results are presented in figure 13 and the differences in slopes of the five curves presented are rather obvious. The early time portions of these curves do not belong to the scaling region. Also, the tails of the curves are influenced by the 'saturation' effects near the gelation boundary and do not belong to the scaling regions either. The average slopes of these curves are determined in the $\log(s)$ region between 3 and 6 units of scale. The resulting

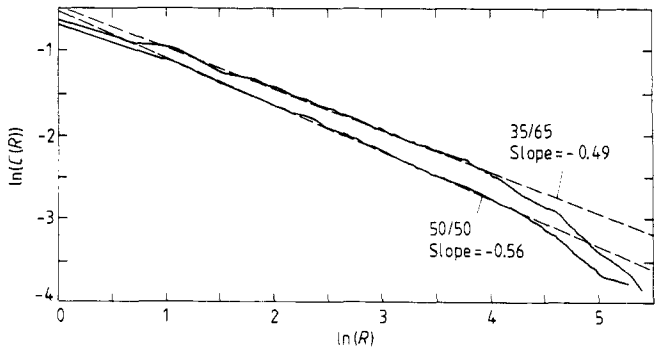

Figure 12. Double logarithmic plot of density-density correlation function $C(R)$ for A_4+B_4 aggregates as a function of the logarithm of distance R. The slope of the curve is equal to the exponent $-\alpha = -(d - D_\alpha)$, where d is the Euclidean dimensionality of the embedding lattice; in this case $d = 2$, and D_α is the fractal dimension of the aggregates. We estimate the fractal dimensionalities to be close to 1.44 for 50% A+50% B and 1.51 for 35% A+65% B system.

Table 1. Radius of gyration exponents (β) and effective dimensionalities $D_\beta (D_\beta = 1/\beta)$ obtained from simulations carried out using the two-dimensional $A_4 + B_4$ model. This was obtained by least-squares fitting straight lines to the coordinates $(\ln(R_g), \ln(s))$ where R_g is the radius of gyration and s is the size of the cluster. Clusters in the size range $s_1 < s < s_2$ were used.

s_1 / s_2		7 / 250	7 / 5000	50 / 5000	25 / 2500
50% A + 50% B	β	0.684 ± 0.012	0.680 ± 0.007	0.673 ± 0.010	0.674 ± 0.004
	D_β	1.46 ± 0.03	1.47 ± 0.02	1.49 ± 0.02	1.48 ± 0.01
35% A + 65% B	β	0.665 ± 0.008	0.662 ± 0.009	0.652 ± 0.024	0.658 ± 0.083
	D_β	1.50 ± 0.02	1.51 ± 0.02	1.53 ± 0.05	1.52 ± 0.17

numbers, representing the effective exponent z as a function of the composition field, are shown in figure 14. The reader should take note both of the fact that the effective exponent z changes with the composition of the mixture and of the functional form of that change.

After an initial period, any aggregating system of a composition close to the optimal contains very few if any free monomers. All that is left are clusters of at least several

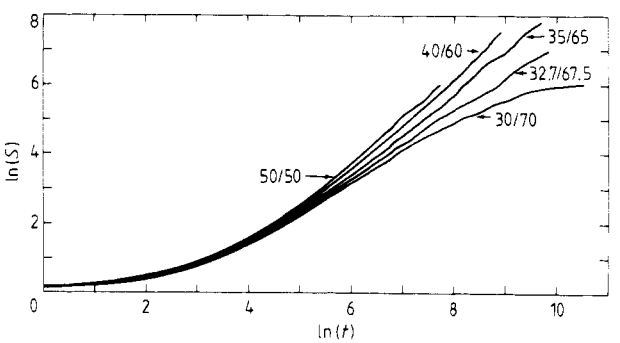

Figure 13. Temporal evolution of the weight average molecular weight $S(t)$ in 2D $A_4 + B_4$ systems of five different compositions indicated by the percentage ratios of A_4 and B_4 monomers.

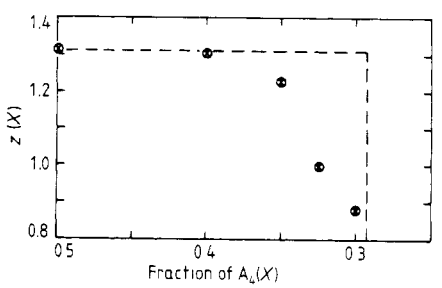

Figure 14. Variation of the effective exponent z with the change of composition of the mixture 2D $A_4 + B_4$. The broken line is the expected behaviour. The position of the edge of the step is not known precisely.

monomers. At that 'advanced' stage of aggregation, systems practically 'forget' that they contain two types of monomers and behave as single-component systems with a sticking probability smaller than one. This is an important conclusion because it allows us to understand why the scaling laws introduced for single-component systems apply to two-component systems.

The recent work of Meakin and Wasserman (1984) demonstrates that a change of sticking probability does not affect the fractal dimension of the aggregates in the cluster-cluster aggregation processes and small sticking probabilities only lead to more compact structures on the small length scales. Large clusters cannot penetrate each other and an increased number of collisions has little effect on the cluster structure on the longer length scales. Again because clusters cannot penetrate each other (Meakin 1984), the fractal dimension of the cluster trajectory has only a very small effect on the fractal character of the cluster-cluster aggregates. The value ($D = 1.53 \pm 0.05$) we obtain for the effective fractal dimensionality of the two-dimensional 35% A_4 + 65% B_4 system is quite similar to that obtained recently by Botet and Jullien (1984) from a cluster-cluster aggregation model in the *limit* of zero sticking probability.

In general, we expect to find a crossover from the fractal dimensionality characteristic of cluster-cluster aggregation with zero sticking probability (Botet and Jullien 1984) ($D = 1.55$ for $d = 2$ and $D = 2.0$ for $d = 3$), on the short length scales, to that characteristic of cluster-cluster aggregation with a large sticking probability ($D = 1.43$ for $d = 2$ and $D = 1.75$ for $d = 3$), on the longer length scales.

If the fractal dimensionality D were independent of the sticking probability p, the time exponent z should be independent as well. The results shown in figure 14 support this conclusion. To appreciate this one should note that the curve $z(x)$ is very flat for small deviations from the symmetric composition and changes rather abruptly towards the end of the gelation region. The same dependence of an effective exponent as a function of an 'irrelevant' field is observed whenever we have a crossover from the critical to tricritical behaviour (Riedel and Wegner 1972). If our measurements of exponent z were made at 'infinite' aggregation times in very large systems, the resulting exponents would be the same for all compositions within the gelation region and would take on a different value only at the boundary composition. The necessity that a scaling field (in this case composition X) takes a precisely selected value, in order that a certain new type of critical behaviour occurs, is an essential feature of the tricritical point. The fact that we observe a smoothly varying curve instead of a step function is the consequence of the finite observation time which is in our simulations directly related to the finite size of the system.

7. Non-gelling region and oligomer formation

At compositions in the gelation region, aggregation always results in the formation of a single large cluster. Beyond that region, several or many clusters are formed. The boundaries of the gelation region therefore delineate two very different types of physical behaviour. To illustrate this difference we have presented in figure 15 the temporal evolution of the $N_s(t)$ cluster numbers of a non-gelling 30% A_2 + 70% B_6 system. These curves should be compared with the results for a gelling mixture given in figure 9. Apparently in a mixture with an overabundance of one kind of monomer, the time evolution of the cluster sizes is characterised by the appearance of the stable small clusters, oligomers. The selection of the surviving cluster sizes reflects the functionality

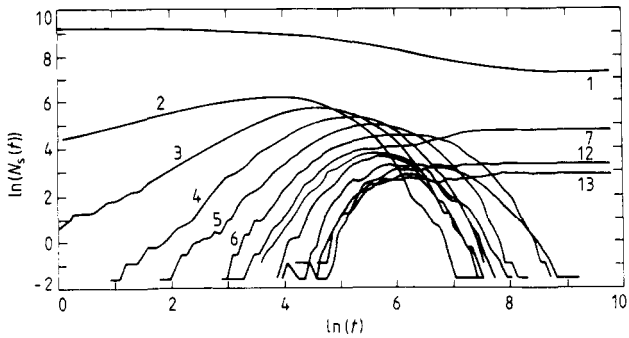

Figure 15. Time dependence of the cluster numbers of 3D 85% A_6+15% B_6 system with a majority of A_6 monomers. Cluster sizes 1, 7, 12 and 13 are saturation points of the distribution.

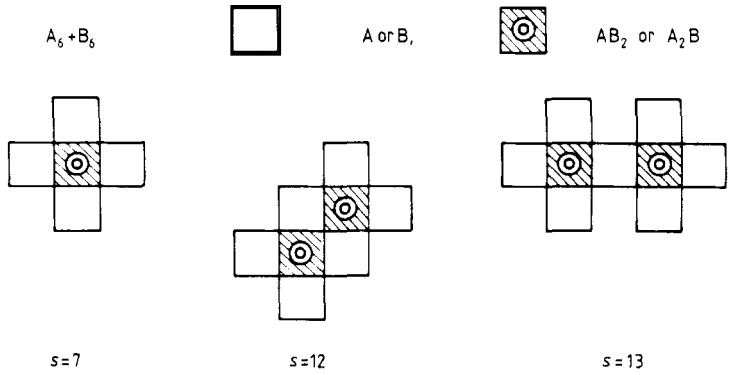

Figure 16. Shapes of the small clusters saturated with A_6 monomers of a 3D A_6+B_6 mixture. Both white and shaded squares are projections of the corresponding three-dimensional cubes representing the six functional monomers.

of monomers and the geometry of the underlying lattice. As an illustration of the oligomers selected by these geometric rules we present in figure 16 the smallest clusters which can be obtained in an A_6+B_6 mixture saturated with A_6 monomers.

A very similar situation takes place in any of the non-gelling regions of all other types of monomer mixtures considered. The relevance of these observations for the real polymer systems will be discussed elsewhere.

8. Discussion

In this paper we have presented some of the results obtained from a new model for polymerisation of multifunctional monomers. Our model automatically includes the same sort of complex geometric effects that are found in real systems. However, the details of these goemetric effects are to some extent dictated by the lattices used in our simulations. Off-lattice simulations should be possible but would require very long computer times and would be relatively difficult to program. In its present form, our model assumes that the aggregation kinetics are diffusion limited. It would be easy to include the effects of finite reactivity via sticking probabilities for A–B interactions,

but again much longer computer times would be required. It should also be easy to extend our model to the aggregation of monomers with mixed functional groups of the A_fB_g type. These simulations are in progress.

One of the major deficiencies of our model which makes it unrealistic for many real systems is that we assume that the clusters, once formed, are completely rigid. We have begun to explore the effects of the structural readjustments after two clusters have contacted each other (Meakin and Jullien 1986) but we still have a long way to go before completely realistic models are available.

Our models produce many of the qualitative features associated with condensation polymerisation in real systems formed from polyfunctional monomers. In particular, we observe the existence of gelling and non-gelling regions of compositions and suggest that the boundaries between these regions are *tricritical* points.

The formation of stable oligomeric structures in the non-gelling region is a novel feature which is not present in the single-monomer cluster-cluster aggregation model. Perhaps one of the most important results of our work is the observation that polymerisation kinetics in the gelling region can be described in terms of the same sort of scaling behaviour as that found recently in cluster-cluster aggregation (Meakin *et al* 1985b, Botet and Jullien 1984) and previously for other systems (Friedlander 1960, 1977, Lushnikov 1973, Silk and White 1978). The dynamic scaling form $N_s(t) = s^{-2}f(s/t^z)$ appears to be quite general and applicable to a very wide range of aggregation and polymerisation processes. It is most likely that modifications of our model such as the inclusion of finite sticking probabilities and internal reorganisation processes will change the scaling exponent z and the scaling function $f(x)$. However, the general scaling form will probably be preserved. This suggests that attempts should be made to apply the above scaling form to experimental systems as well as to other simulations.

References

Ball R and Witten T A 1983 unpublished
Botet R and Jullien R 1984 *J. Phys. A: Math. Gen.* **17** 2517
Deutch J M and Meakin P 1983 *J. Chem. Phys.* **78** 2093
Djordjević Z B 1984 *PhD Thesis* MIT, Cambridge
Djordjević Z B and Meakin P 1986 to be published
Feder J, Jossang T and Rosenquist E 1984 *Phys. Rev. Lett.* **53** 1403
Flory P J 1953 *The Principles of Polymer Chemistry* (Ithaca, NY: Cornell University Press)
Forrest S R and Witten T A 1979 *J. Phys. A: Math. Gen.* **12** L109
Friedlander S K 1960 *J. Meteorol.* **17** 479
Friedlander S K 1977 *Smoke, Dust and Haze: Fundamentals of Aerosol Behavior* (New York: Wiley)
Kang K and Redner S 1984 *Phys. Rev. Lett.* **52** 955
Kinzel W and Yeomans J M 1981 *J. Phys. A: Math. Gen.* **14** L163
Kolb M 1984 *Phys. Rev. Lett.* **53** 1653
Kolb M, Botet R and Jullien R 1983 *Phys. Rev. Lett.* **51** 1123
Kolb M and Jullien R 1984 *Preprint*
Lushnikov A A 1973 *J. Colloid Interface Sci.* **45** 549
Mandelbrot B B 1982 *The Fractal Geometry of Nature* (San Francisco: Freeman)
Meakin P 1983 *Phys. Rev. Lett.* **51** 1119
—— 1984 *Phys. Rev.* A **29** 997
Meakin P, Cheng Z Y and Deutch J M 1985a *J. Chem. Phys.* **XX**
Meakin P and Jullien R 1986 to be published
Meakin P, Vicsek T and Family F 1985b *Phys. Rev.* B **31** 564

Meakin P and Wasserman Z R 1984 *Phys. Lett.* **103A** 337
Meakin P and Witten T A 1983 *Phys. Rev.* B **28** 5632
Nakanishi H and Reynolds P J 1978 *Phys. Lett.* **71A** 252
Racz Z and Plishke M 1984 *Phys. Rev. Lett.* **53** 415
Riedel E K and Wegner F J 1972 *Phys. Rev. Lett.* **29** 349
Silk J and White S D 1978 *Astrophys. J.* **22** L59
Sutherland D M and Goodarz-Nia I 1971 *Chem. Eng. Sci.* **26** 2071
Vicsek T and Family F 1984 *Phys. Rev. Lett.* **52** 1669
von Schulthess G K, Benedek G B and DeBlois R W 1980 *Macromol.* **13** 939
Weitz D A and Oliveria M 1984 *Phys. Rev. Lett.* **52** 1433
Witten T A and Sander L M 1981 *Phys. Rev. Lett.* **47** 1400
Ziff R M, Hendriks E M and Ernst M H 1982 *Phys. Rev. Lett.* **43** 593